BioMedical Engineering OnLine

RESEARCH

Open Access

A KNN-based model for non-invasive prediction of hemorrhagic shock severity in prehospital settings: integrating MAP, $P_{BU}CO_2$, $P_{TC}O_2$, and PPV

Peng Zhao[1*], Wencai Pan[2], Xin Zou[2], Jiaqing Yang[2], Shihui Zhang[2], Yufei Liu[3] and Yang Li[4]

*Correspondence:
zhaop9@gmail.com

[1] Chongqing Hospital, Union Hospital, Tongji Medical College, Huazhong University of Science and Technology, No. 799, Liangjiang Avenue, Longxing Town, Yubei District, Chongqing 401121, China
[2] Department of Medical Engineering, Xinqiao Hospital Army Medical University, Chongqing 400037, China
[3] Key Laboratory of Optoelectronic Technology & Systems, Ministry of Education, (Chongqing University), Chongqing 400044, China
[4] State Key Laboratory of Trauma, Burns and Combined Injuries, Medical Center of Trauma and War Injury Daping Hospital, Army Medical University, Chongqing 400042, China

Abstract

Background: Rapid prehospital assessment of hemorrhagic shock severity is critical for trauma triage and intervention. Current non-invasive single-parameter monitoring shows limited diagnostic reliability. We developed a multi-parameter predictive model integrating mean arterial pressure (MAP), buccal mucosal CO_2 ($P_{BU}CO_2$), transcutaneous oxygen ($P_{TC}O_2$), and pulse pressure variation (PPV). using K-nearest neighbors (KNN) algorithm.

Methods: Forty-five Wistar rats were randomly divided into five groups ($n=9$) with different blood loss amounts. MAP, $P_{BU}CO_2$, $P_{TC}O_2$, and PPV measurements were continuously obtained. A multi-parameter shock severity prediction model was established based on the KNN algorithm. Leave-one-out cross-validation was used to determine the value of *K*. Meanwhile, a prediction model based on the support vector machine (SVM) algorithm was established. The performance of the two prediction models was compared using confusion matrices and receiver operating characteristic (ROC) curve.

Results: When the training vs testing data set ratio is 7:3 or 6:4, and $K=3$, the KNN-based model has the best prediction accuracy (94.82% and 93.51%). The confusion matrix and ROC evaluation showed that the overall performance of the KNN-based model is superior to that of the SVM-based model, at all levels of blood loss (F1 = 95.09% and 93.99%, AUC = 1 and 0.97 for the KNN-based model at 7:3 and 6:4 dataset ratio; F1 = 83.84% and 84.86%, AUC = 0.97 and 0.97 for the SVM-based model at 7:3 and 6:4 dataset ratio).

Conclusions: Using the detection indicators MAP, $P_{BU}CO_2$, $P_{TC}O_2$ and PPV, the KNN-based rat hemorrhagic shock severity prediction model has high accuracy and stability, and demonstrates potential feasibility for severity stratification of hemorrhagic shock in standardized preclinical models, providing a foundation for future clinical validation in prehospital environments.

Keywords: K-nearest neighbor algorithm, Hemorrhagic shock, Multi-parameter, Prediction model

Introduction

Hemorrhagic shock (HS) is a common complication after traumatic injury [1]. Fast and effective assessment of the severity of blood loss in the injury before reaching the hospital can be of significant importance in triage and early treatment of the patient. Generally, the clinical diagnosis for the severity of hemorrhagic shock is by monitoring heart rate (HR), blood pressure, urine volume, mental status, skin color and other indicators [2–4]. Yet, in the early stage of shock, these indicators cannot truly reflect the severity of shock due to compensatory effects. Moreover, the symptoms of pale skin, low blood pressure and reduced urine volume are not symptoms specific of hemorrhagic shock [5]. Cardiac output (CO) is one of the more sensitive indicators of hemorrhagic shock. However, accurate measurement of CO depends mainly on invasive detection, which limits its application in prehospital situations. Arterial blood lactate (ABL) has been widely recognized as the "gold standard" indicator for the late diagnosis of hemorrhagic shock [6]. However, ABL cannot be non-invasively monitored continuously, and therefore is not suitable for guiding resuscitation during prehospital first aid or during transit. Especially in natural disasters (e.g., earthquake), traffic accidents or in combat situations, the limitations of the above-mentioned detection indicators present challenges to medical personnel to effectively assess the severity of shock in patients during the "critical time". This can result in inaccurate classification of injuries, delayed transport and inappropriate recovery plan. In recent years, much research effort has been put into finding a method for evaluating the severity of hemorrhagic shock before hospitalization.

Current methods for prehospital evaluating the severity of hemorrhagic shock are mainly based on non-invasive detection of hemodynamics and oxygen metabolism indicators [7–9]. In prehospital settings, however, the ECG waveforms are susceptible to factors such as edema, body position, noise, etc. In contrast, pulse pressure variation (PPV) is proven less affected by the environment and the availability of their non-invasive measurement renders them much preferable to other indicators in prehospital setting, and it is defined by the difference between the maximal and minimal pulse pressure divided by the mean of these two values and is determined over one breathing cycle. However, the data of PPV obtained by non-invasive method suffers from relatively low accuracy at lower blood volume [10]. The compensatory reserve index (CRI) can accurately quantify the severity of shock [4, 11], but its calibration requires a large sample size, and is susceptible to the effects of individual differences. In contrast to hemodynamic indicators, oxygen metabolism indicators can directly reflect microcirculation and tissue perfusion, and the evaluation of shock severity using these indicators is more direct and effective [12, 13]. Buccal mucosal CO_2 partial pressure ($P_{BU}CO_2$) is the most sensitive non-invasive detection indicator for oxygen metabolism. Its use in the quantitative evaluation of the severity of hemorrhagic shock has been widely recognized [14]. However, the sensor for $P_{BU}CO_2$ detection is large and is susceptible to factors such as oral temperature and microenvironment [15]. Thus, all the above-mentioned individual non-invasive detection indicators each has its limitations, and cannot accurately reflect the true situation of hemorrhagic shock. Therefore, some studies have tried to use a combination of several non-invasive detection indicators to establish a new method for the fast, accurate and quantitative assessment of hemorrhagic shock severity before hospitalization [16, 17].

The multi-parameter model, leveraging physiological complementarity and feature interaction, enables comprehensive coverage of disease pathology and supports more accurate clinical decision-making [18, 19]. Recent reports have established multi-parameter prediction models for hemorrhagic shock evaluation using logistic regression (LR), neural networks (NN), random forest (RF), and support vector machines (SVM), etc., and have obtained high accuracy [20–22]. Kim et al. used multiple detection indicators to establish a mortality prediction model with variable selection, and indicated that the SVM-based model with blood lactate concentration (LC) and a new hemorrhage-induced severity index (NI, NI = LC/perfusion index (PI)) as important variables had better sensitivity (1.000) and area under curve (0.972) than the LR, NN and RF models [20]. Choi et al. also attempted to compare three popular machine learning algorithms using NI, PI, diastolic blood pressure (DBP) and mean arterial pressure (MAP) as the optimal variables for predicting the Advanced Trauma Life Support hemorrhagic shock class in rats, and confirmed that the SVM-based model had the highest accuracy of 80.8% [21]. Further, Natasa et al. established the SVM-based model for discriminating between hypovolemia and euvolemia using photoplethysmography (PPG) signals of the human body, and obtained the best overall accuracy of 88.38% [22]. However, of the indicators used, PPG are difficult to measure in prehospital setting due to motion artifacts and insufficient perfusion (such as shock) in patients in the pre-hospital scene, skin dirt, vasoconstriction caused by sweating or cold exposure, etc. [23, 24], the SVM-based model has not yet used the key oxygen metabolism indicators, which may be the reason for its low accuracy.

Our previous work has been focused on the method of combining hemodynamic and oxygen metabolism indicators to evaluate the hemorrhagic shock severity. We were also based on the commonly used clinical indicators MAP, HR, $P_{BU}CO_2$, and shock index (SI = HR/systolic and diastolic blood pressures), to establish a SVM-based model in rats, and obtained higher accuracy (90.88%), but the reliability was worse [25]. In the present work, we improved the non-invasive measurement method of $P_{BU}CO_2$ and introduced transcutaneous oxygen partial pressure ($P_{TC}O_2$) which is an oxygen metabolism indicator suitable for prehospital detecting, and used PPV instead of HR and SI. And we hypothesized that the K-nearest neighbor (KNN) algorithm in the advantage of small sample size, multi-modal and nonlinear classification would achieve higher accuracy and reliability than current methods in the multi-parameter prediction model, using the above-mentioned four indicators of hemorrhagic shock severity in rats. We also tested the accuracy, overall performance and comprehensive prediction ability of our KNN-based model against the SVM-based model for validation.

Results

Dataset

The data collected by the experiment are normally distributed. Table 1 shows the baseline of the experimental data. There were no significant baseline differences in the same physiological indicators (MAP, $P_{BU}CO_2$, $P_{TC}O_2$, or PPV) between different groups of rats. The four physiological indexes (MAP, $P_{BU}CO_2$, $P_{TC}O_2$ and PPV) measured at 15 min intervals in each blood loss group are shown in Fig. 1. Table 2 shows the statistical comparison results. As shown in Table 2, the differences are significant, both between

Table 1 Baseline characteristics

Group	n	MAP	$P_{BU}CO_2$	$P_{TC}O_2$	PPV
Sham	9	112.67 ± 9.22	35.03 ± 1.72	62.50 ± 5.48	5.60 ± 2.21
25% blood loss	9	132.00 ± 7.21	34.03 ± 1.35	65.00 ± 6.49	6.17 ± 2.42
30% blood loss	9	130.00 ± 10.00	34.67 ± 1.72	62.83 ± 4.16	4.57 ± 0.40
35% blood loss	9	123.00 ± 7.00	35.50 ± 1.35	60.77 ± 6.55	6.13 ± 1.86
40% blood loss	9	120.00 ± 6.46	35.63 ± 1.16	62.30 ± 4.69	4.60 ± 1.57

All data are presented as mean ± SD

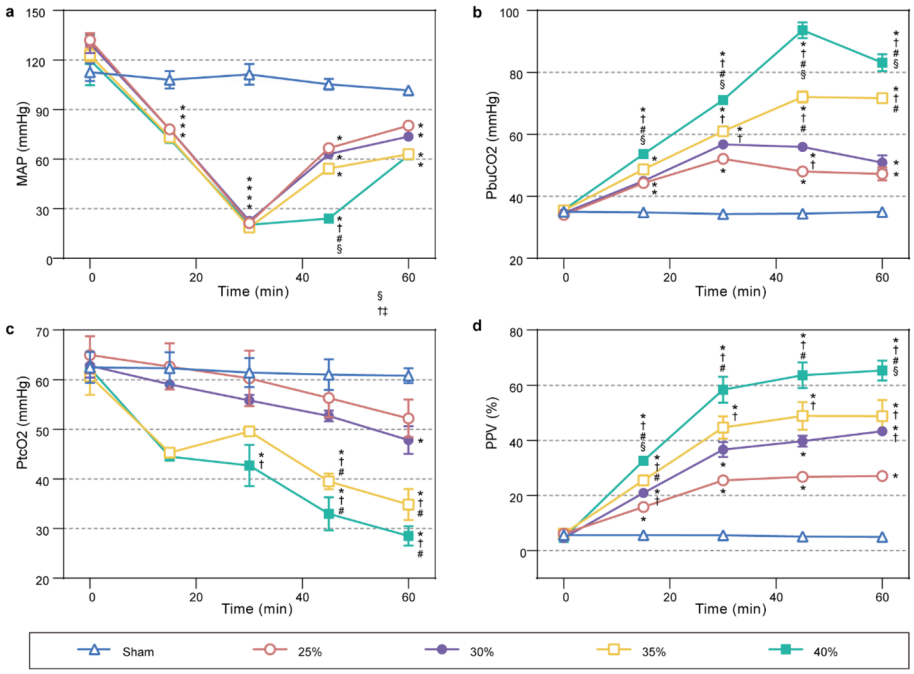

Fig. 1 Measurement of the four physiological indicators in different blood loss groups over time. (**a**) MAP. (**b**) $P_{BU}CO_2$. (**c**) $P_{TC}O_2$. (**d**) PPV. All data are presented as mean ± SD. 25%, 30%, 35% and 40% vs sham, $^{*}p < 0.05$; 30%, 35% and 40% vs 25%, $^{\dagger}p < 0.05$; 35% and 40% vs 30%, $^{\#}p < 0.05$; 40% vs 35%, $^{\S}p < 0.05$

Table 2 *F* and *P* values of ANOVAs

Factors	Variables	*F* Value	*P* Value
MAP	Group	18.079	< 0.001
	Time	297.786	< 0.001
	Group*Time	12.915	< 0.001
$P_{BU}CO_2$	Group	168.284	< 0.001
	Time	1207.186	< 0.001
	Group*Time	191.837	< 0.001
$P_{TC}O_2$	Group	6.964	< 0.001
	Time	892.411	< 0.001
	Group*Time	89.913	< 0.001
PPV	Group	54.769	< 0.001
	Time	444.178	< 0.001
	Group*Time	46.308	< 0.001

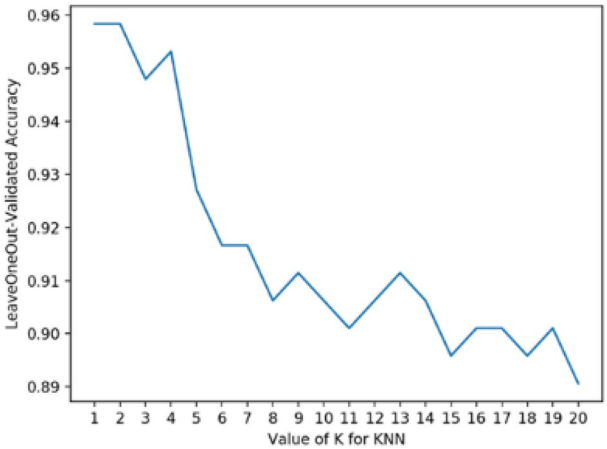

Fig. 2 Classification accuracy at different *K* values

Table 3 Classification accuracy at different *K* values and different training vs test set ratios

K Value	Training set vs testing set								
	9:1	**8:2**	**7:3**	**6:4**	**5:5**	**4:6**	**3:7**	**2:8**	**1:9**
3	100	89.74	94.82	93.51	84.38	81.03	80	76.62	73.99
4	100	92.31	89.66	90.91	85.42	83.62	80.74	77.27	73.99

groups and between time points, in all four physiological indexes ($p < 0.001$). There is also interaction between grouping and time ($p < 0.001$). Based on this, all data can be used to build the data set.

Determination of model parameters

KNN-based prediction model

The value of K was varied from 1 to 20. Figure 2 shows the accuracy measured by the leave-one-out validation method for each K value. It is shown that when the $K \leq 4$, this model provides classification with high accuracy. Considering that the K value must not be too small, we took the K value of 3 and 4, and further tested the classification accuracy by varying the training set to test set ratio. The results are shown in Table 3. It can be seen that when training vs test set ratio is larger than 1, the classification accuracy can reach higher than 90%. In practical model building, K is usually an odd number, so as to avoid ambiguity. Therefore, in this study, the K value was set as 3.

Multi-parameter prediction model based on the SVM algorithm

In the SVM model, the penalty parameter C was set as 1, and the γ parameter is the inverse of the feature space dimension (i.e., levels of blood loss), 1/4.

Validation of the classification results

Due to limited sample size, setting the ratio of the training set to test set too high is likely to cause overfitting. Therefore, we tested accuracy of our classification models using the training vs test set ratios of 7:3 and 6:4. As shown in Table 3, when $K = 3$, the KNN-based

classification model has an accuracy of 94.82% (at 7:3) or 93.51% (at 6:4), while SVM-based classification model has an accuracy of 82.76% (at 7:3) or 84.42% (at 6:4). It shows that the KNN-based classification model achieved a higher accuracy than does the SVM-based classification model.

Evaluation result using confusion matrix

The normalized confusion matrices of the KNN- and SVM- based models at the two data set ratios are shown in Fig. 3, where the columns are the actual classification and the rows are the predicted classification. The precision, recall, and F1-score of the two models at 7:3 and 6:4 data set ratios were derived from Fig. 3, and are presented in Tables 4 and 5, respectively.

The KNN-based model has higher accuracy than the SVM-based model at the 25% and 35% blood loss level, and the SVM-based model has a higher accuracy at the 30% blood loss level. Overall, the average accuracy using the KNN-based model, 95.45% (at 7:3) or 94.23% (at 6:4), is higher than using the SVM-based model, which is 87.35% (at 7:3) or 88.10% (at 6:4), respectively.

At all levels of blood loss, the KNN-based model has a recall rate higher than the SVM-based model. The average recall rate of all blood loss levels using the KNN-based model is 95.06% (at 7:3) or 94% (at 6:4).

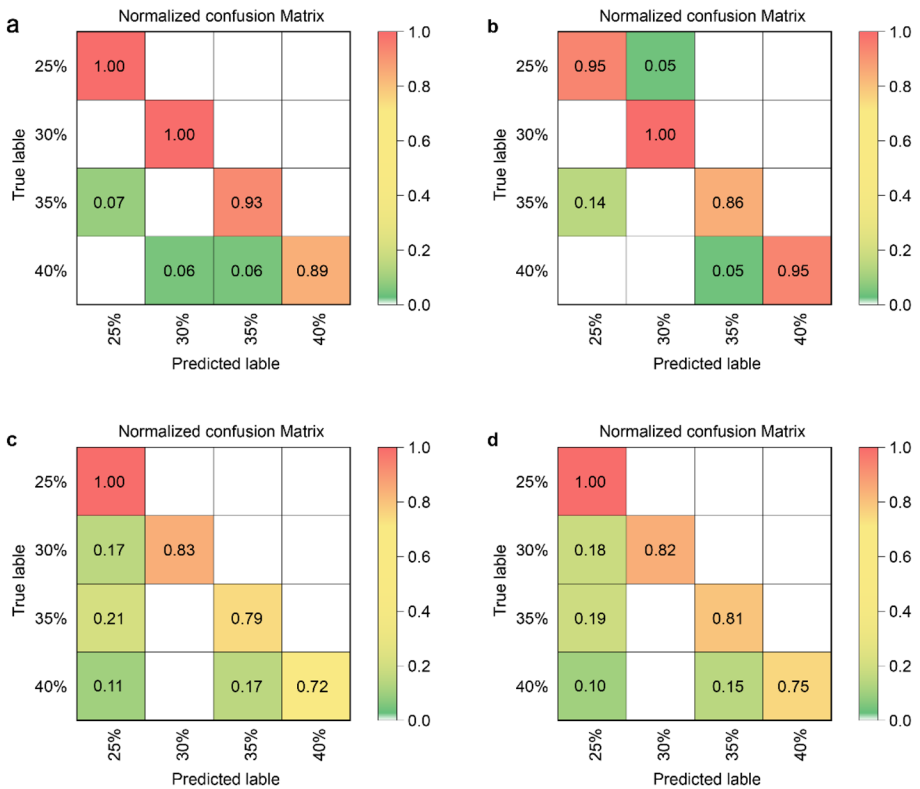

Fig. 3 Normalized confusion matrices for the KNN- and SVM- based multi-parameter prediction models. (**a**) confusion matrix for the KNN-based model at 7:3 data set ratio. (**b**) confusion matrix for the KNN-based model at 6:4 data set ratio. (**c**) confusion matrix for the SVM-based model at 7:3 data set ratio. (**d**) confusion matrix for the SVM-based model at 6:4 data set ratio

Table 4 Precision, Recall rate and F-1 score of the KNN- and SVM- based models at the training vs test set ratio of 7:3

Group	KNN			SVM		
	Precision (%)	Recall (%)	F1-score (%)	Precision (%)	Recall (%)	F1-score (%)
25% blood loss	93.46	100	96.62	67.11	100	80.32
30% blood loss	94.34	100	97.09	100	83	91.71
35% blood loss	93.94	93	93.47	82.29	79	80.61
40% blood loss	100	87.25	93.19	100	72	83.72
avg/total	95.45	95.06	95.09	87.35	83.50	83.84

Table 5 Precision, Recall rate and F-1 score of the KNN- and SVM- based models at the training vs test set ratio of 6:4

Group (%)	KNN			SVM		
	Precision (%)	Recall (%)	F1-score (%)	Precision (%)	Recall (%)	F1-score (%)
25% blood loss	87.16	95	91.08	68.03	100	84.02
30% blood loss	95.24	100	97.62	100	82	91.00
35% blood loss	94.51	86	90.26	84.38	81	82.69
40% blood loss	100	95	97.50	100	75	87.5
avg/total	94.23	94	94.12	88.10	84.50	86.30

The average F1-score of all blood loss levels using the KNN-based model is 95.09% (at 7:3) or 93.99% (at 6:4), higher than the average F1-score of all blood loss levels using the SVM-based model (83.84% and 84.86%, respectively). These results indicate that the KNN-based classification model has superior performance over the SVM-based model.

Evaluation results using ROC curve and AUC

The ROC curves and AUCs for the KNN-based model and the SVM-based model at data ratio of 7:3 and 6:4 are shown in Fig. 4.

Compared to the SVM-based model, the individual and the average ROCs of the KNN-based model are closer to the top left corner, especially when the training to test set ratio is 7:3. This shows that the KNN-based multi-parameter prediction model performed better than did the SVM-based model, in both individual and overall classification.

As shown in Fig. 4a and b, the AUC of prediction accuracy using the KNN-based model was 1.00, 1.00, 1.00 and 1.00 for 25%, 30%, 35%, and 40% blood loss, respectively, at 7:3 training to test set ratio, and 0.97, 1.00, 0.92 and 1.00, respectively, at 6:4 training to test set ratio. The micro- and macro- averaged AUCs are 1.00 and 1.00 (at 7:3 data set ratio), respectively, and 0.97 and 0.97 (at 6:4 data set ratio), respectively.

As shown in Fig. 4c and d, the AUC of prediction accuracy using the SVM-based model was 0.97, 0.99, 0.93, and 0.97 for 25%, 30%, 35%, and 40% blood loss, respectively, at 7:3 training to test set ratio, and 0.96, 0.99, 0.90 and 0.99, respectively, at 6:4 training to test set ratio. The micro- and macro- averaged AUCs are 0.97 and 0.97 (at 7:3 data set ratio), respectively, and 0.96 and 0.97 (at 6:4 data set ratio), respectively.

The above results demonstrated that, the overall performance of the KNN-based model is superior to the SVM-based model. Especially when the training to test data set

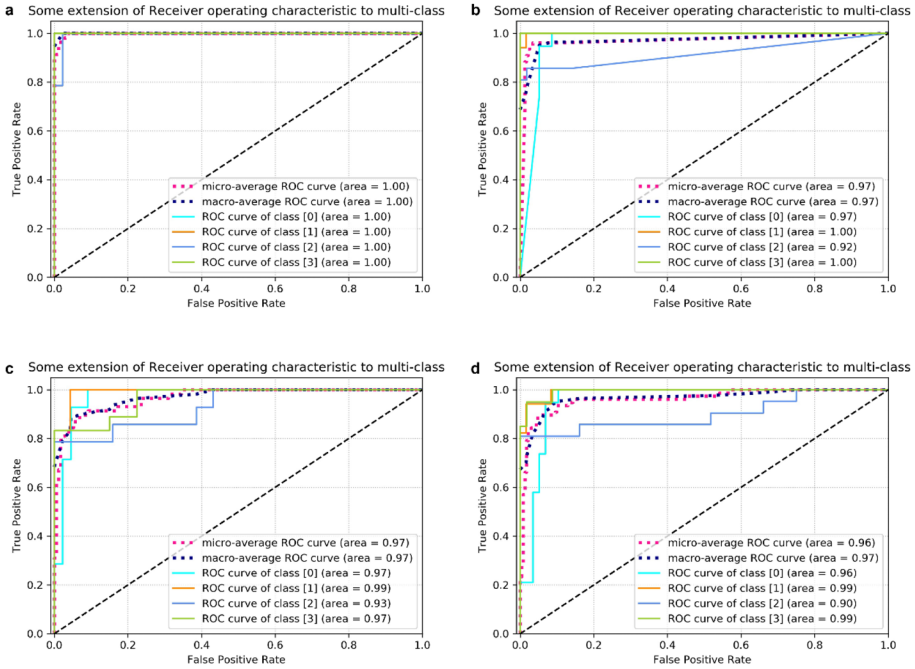

Fig. 4 ROC curve and AUC evaluation for the KNN- and SVM- based models at 7:3 and 6:4 training to test set ratios. (**a**) ROC curve and AUC evaluation for the KNN-based model at 7:3 data set ratio. (**b**) ROC curve and AUC evaluation for the KNN-based model at 6:4 data set ratio. (**c**) ROC curve and AUC evaluation for the SVM-based model at 7:3 data set ratio. (**d**) ROC curve and AUC evaluation for the SVM-based model at 6:4 data set ratio. class [0], 25% blood loss; class [1], 30% blood loss; class [2], 35% blood loss; class [3], 40% blood loss

ratio is 7:3, the AUC is 1 for both individual and average ROC curves, showing excellent performance of the KNN-based model.

Discussion

To our knowledge, this study is the first to use MAP, $P_{BU}CO_2$, $P_{TC}O_2$ and PPV as physiological indicators for the establishment of a KNN- or SVM- based multi-parameter hemorrhagic shock severity prediction model. Using controlled hemorrhagic shock in rats as animal model, the KNN-based model achieved high accuracy: 94.82% at 7:3 data set ratio, and 93.51% at 6:4 data set ratio, which are higher than the accuracy of the SVM-based model. Evaluation by confusion matrix and by ROC curve showed that the KNN-based model has higher F1-score (95.09 at 7:3 data set ratio and 94.12 at 6:4 data set ratio) compared to the SVM-based model (83.84 at 7:3 data set ratio and 84.86 at 6:4 data set ratio), and higher AUC (1.00 at 7:3 data set ratio and 0.97 at 6:4 data set ratio) compared to the SVM-based model (0.97 at both 7:3 and 6:4 data set ratio). These results provide support that the KNN-based hemorrhagic shock severity prediction model has higher accuracy and better overall performance than the SVM-based model.

The four non-invasive physiological indicators in this prediction model are, hemodynamic indicators MAP and PPV, and oxygen metabolism indicators $P_{BU}CO_2$ and $P_{TC}O_2$. As this study, in the hemorrhagic shock model, the mean MAP of the four groups with different blood loss amounts all showed similar downward trajectories, approached 30 mmHg at approximately 30 min, and the MAP rebounded after 30

min. After hemorrhagic shock occurs, MAP can quickly reflect changes in blood volume and CO, and the amount of MAP decrease is positively correlated to the amount of blood loss [26]. Clinically, it is a widely used indicator to guide fluid resuscitation [27, 28]. However, due to the compensatory mechanism, the change in MAP is not significantly different between mild and moderate hemorrhagic shock [29]. While PPV has a high level of linear correlation with the amount of blood loss and is an indicator that can be easily obtained in prehospital environment using non-invasive method, the accuracy of its measurement is limited by current non-invasive blood pressure measurement techniques [30, 31]. The essence of shock is hypoxia of tissue cells, which further causes damage such as severe microcirculation dysfunction, tissue hypoperfusion, etc. Clinical studies have shown that the CO_2 content in tissues can reflect cellular oxygen metabolism, and is helpful in determining tissue hypoperfusion and guiding fluid resuscitation [32–34]. $P_{BU}CO_2$ is proven to be the most sensitive non-invasive oxygen metabolism indicator that reflects hemorrhagic shock [14, 15, 35]. It has high correlation with other physiological parameters such as ABL, ABP, and BD. Our research group has devoted much effort in developing non-invasive measurement methods for $P_{BU}CO_2$ [15]. Recently, using the MEMS technology, we developed a new type of nano CO_2 sensor that can be attached to the epidermis, which overcomes the problems of existing electrochemical based CO_2 micro sensors – low accuracy, poor stability and difficulty in fixation. Meanwhile, $P_{TC}O_2$ is a clinically mature, easily accessible non-invasive oxygen metabolism indicator, yet it can only reflect the oxygen content of local tissue microcirculation, and cannot fully replace the "gold standard", the partial pressure of oxygen in arterial blood (PaO_2), which is an invasive indicator. The above-mentioned physiological indicators reflect different aspects of the hemorrhagic shock pathology, yet each individual indicator has its own limitations. Therefore, effective integration of these indicators in the comprehensive evaluation of hemorrhagic shock severity, with good accuracy and consistency, will be of significant clinical value in the early diagnosis and treatment of hemorrhagic shock.

Literature evidence shows that the accuracy of SVM is higher than that of other popular machine learning algorithm models [21], but the KNN algorithm has strong adaptability to small sample data [36, 37]. Given the limited sample size of this study, we adopted SVM and KNN for double validation. The verification results show that both the models based on KNN and SVM can predict the severity of hemorrhagic shock, but the accuracy rate of the model based on knn is higher than that of the model based on SVM. These results indicate that the prediction model we proposed in this work has important implications in prehospital quantitative assessment of the severity of hemorrhagic shock, potentially overcoming the limitations of diagnosis relying on a single-indicator. If the detection of the above four indicators is further integrated on a wearable device or multi-functional stretcher with Bluetooth communication, emergency personnel can use mobile terminals (e.g., mobile phones, tablets) to calculate the blood loss through the prediction model, which would provide an assisted decision-making for triage and fluid resuscitation in prehospital setting.

Hemorrhagic shock mostly occurs in natural disasters, accidents, and in battle settings [38]. Fast and accurate quantitative assessment of shock severity is of great significance for improving the success rate of prehospital treatment for trauma patients [39, 40]. The results

from this study have demonstrated that the KNN-based multi-parameter hemorrhagic shock severity model is highly accurate, and showed the feasibility of this method, providing theoretical and technical support for subsequent research on automated and artificial intelligence-driven prehospital rescue and treatment.

There are still limitations to this method, however. First, the data used to establish this multi-parameter prediction model is from a rat model of controlled hemorrhagic shock, while both civilian trauma victims and military combat wounded experienced uncontrolled blood loss before effective hemostasis [41]. In the case, the changes of hemodynamics and oxygen metabolism indicators, and even the mortality rate of shock, will be different from those of the controlled one. Also, differences exist between rat and human circulatory systems. To apply this prediction model to humans, further large-animal models and clinical research are needed to ensure its reliability and safety. Second, this study only used the universal function of the KNN algorithm and SVM algorithms, limited training sample data to establish a prediction model, and verified the accuracy, sensitivity and specificity of the classification, and has not yet compared the differences between different distance functions and large sample training sets. For better robustness, it is necessary to increase the sample size and test more algorithm forms. Third, although there are many validated non-invasive techniques measuring MAP, most of them are specially designed for human rather than rats. Therefore, we applied an invasive pressure sensor in the experiment to obtain information of MAP. In order to bolster confidence in our key finding, further research is required to test whether the model can also achieve good performance when a non-invasive MAP measurement on large animals is implemented. Fourth, the KNN algorithms and the SVM algorithms used in this study are relatively common algorithms in machine learning, while deep learning methods are becoming more mature and effective in multi-modal classification in recent years. Future work can involve using the advantage of the KNN algorithm to prune the training data set, and then build the multi-parameter prediction model based on deep learning methods, such as convolutional neural networks, deep belief networks, recurrent neural networks, etc., to further improve the speed, generalizability and credibility of this classification method while maintaining its high accuracy [42–44]. So that it can be used in clinical practice as soon as possible.

Conclusion

In summary, we established, for the first time, using the four physiological parameters of MAP, $P_{BU}CO_2$, $P_{TC}O_2$ and PPV as non-invasive physiological indicators in prehospital conditions, a multi-parameter prediction model for the severity of hemorrhagic shock based on the KNN algorithm. This model achieved high accuracy in predicting different shock levels, has good feasibility and stability, and demonstrates potential feasibility for severity stratification of hemorrhagic shock in standardized preclinical models, providing a foundation for future clinical validation in prehospital environments.

Materials and methods

Animal experiment

Animal

Forty-five male Wistar rats (Weight: 350 ± 50 g, Experimental Animal Center of Army Military Medical University, Chongqing, China) were housed in specific pathogen-free

(SPF) facilities under controlled environmental conditions, and randomly divided into five groups of equal numbers (n = 9), including a sham group that received only intubation without blood loss. The other four groups were subjected to controlled blood loss of 25%, 30%, 35% and 40% of the calculated total blood volume (Blood loss/total blood volume * 100%; total blood volume (ml) = body weight (g) * 6% [45]) evenly over a 30 min-period. All experimental procedures were approved by the Laboratory Animal Welfare and Ethics Committee of the Third Military Medical University.

Experimental protocol

Prior to experiments, animals were fasted for 12 h with free to drink water. At the beginning of the experiment, the indoor ambient temperature was maintained at 22 ± 2 °C, the humidity was maintained at 55 ± 5%, and the air was purified and disinfected. Surgical procedures took approximately 30 min, followed by a 15-min resting time. 15 min after intubation surgery, controlled bleeding was performed from the left femoral artery at a constant speed for 30 min, and the animals'ECG, MAP, $P_{BU}CO_2$, $P_{TC}O_2$, and pulse wave indicators were continuously monitored for 1 h. The experimental protocol is shown in Fig. 5.

Surgical procedures

Animals were anesthetized by intraperitoneal injection with 4.5% sodium pentobarbital (P3761, Sigma, USA), positioned supine on a thermostatic heating pad (37 ± 0.5 °C), and secured with limbs immobilized. During the surgical procedure, animals were maintained under spontaneous breathing. The abdominal and bilateral groin regions were shaved and disinfected. Two polyethylene (PE 60) catheters were inserted into the left and right femoral arteries, respectively. The left femoral artery catheter was connected via a T-connection to a microinjection pump and a 10 mL syringe. The microinjection pump is used to control bleeding. The syringe was used for heparinization with sodium heparin solution (2 ml/kg). The right femoral artery catheter was connected to a pressure sensor (MLT0380, AD Instruments, Bella Vista, Australia) for blood pressure measurement. A flexible micro-nano CO_2 sensor, developed in our lab using micro-electromechanical systems (MEMS) technology, was applied to the buccal mucosa to non-invasive measure $P_{BU}CO_2$. Four transcutaneous sensors (E5250, Radiometer, Copenhagen, Denmark) were connected to a base mounted on the abdomen with double-sided tape, to

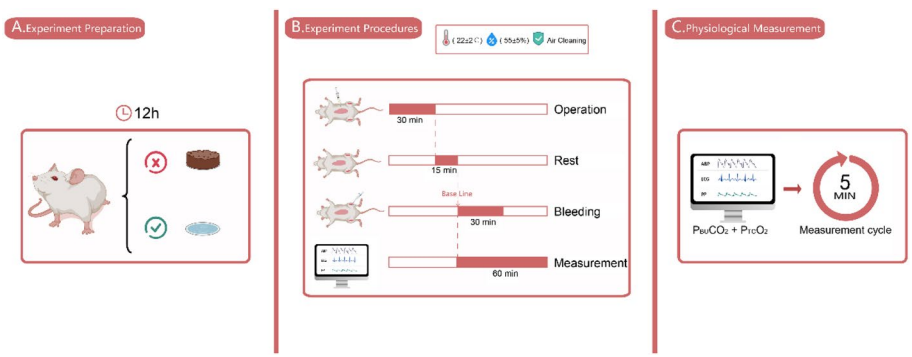

Fig. 5 Diagram of the experimental protocol

non-invasive measure $P_{TC}O_2$. A pulse sensor (MLT125/R, AD Instruments, Bella Vista, Australia) was secured around the animal's tail to non-invasive measure pulse. The ECG was measured by the II lead method, with the positive electrode, the negative electrode, and the ground wire attached to the left lower limb, the right upper limb, and the right lower limb, respectively. The experimental scheme is shown in Fig. 6.

Physiological measurements

We developed the new micro-nano CO_2 sensor composed of a 3 ×3 silicone-based micro-nano needle array and a silicone flexible base (Fig. 7a). The micro-nano needle array was attached to the flexible silicone base via a silicone adhesive and packaged with parylene C and polydimethylsiloxane. Each micro-nano needle is coated with two different concentrations of solid $NaHCO_3$ on its two sides, respectively, and each side is embedded with a platinum electrode and wire (Fig. 7b). The HCO_3^- concentrations on the two sides of the micro-nano needle (A and B) are set as such that the CO_2 concentration to be measured (Y), falls in between, i.e., $B < Y < A$. When the concentrations at the micro-nano needles and in the mucus reach equilibrium, the H^+ on the two sides of the micro-nano needle would generate potentials E1 and E2, respectively, and form a difference in potential ΔE (Fig. 7c). Consequently, Y can be derived using the Nernst equation.

Real time monitoring of hemodynamic parameters ECG, MAP, and PPV were performed using the POWERLAB Data Acquisition and Analysis System (PL3508, AD Instruments, Bella Vista, Australia). The ECG electrode was connected to the

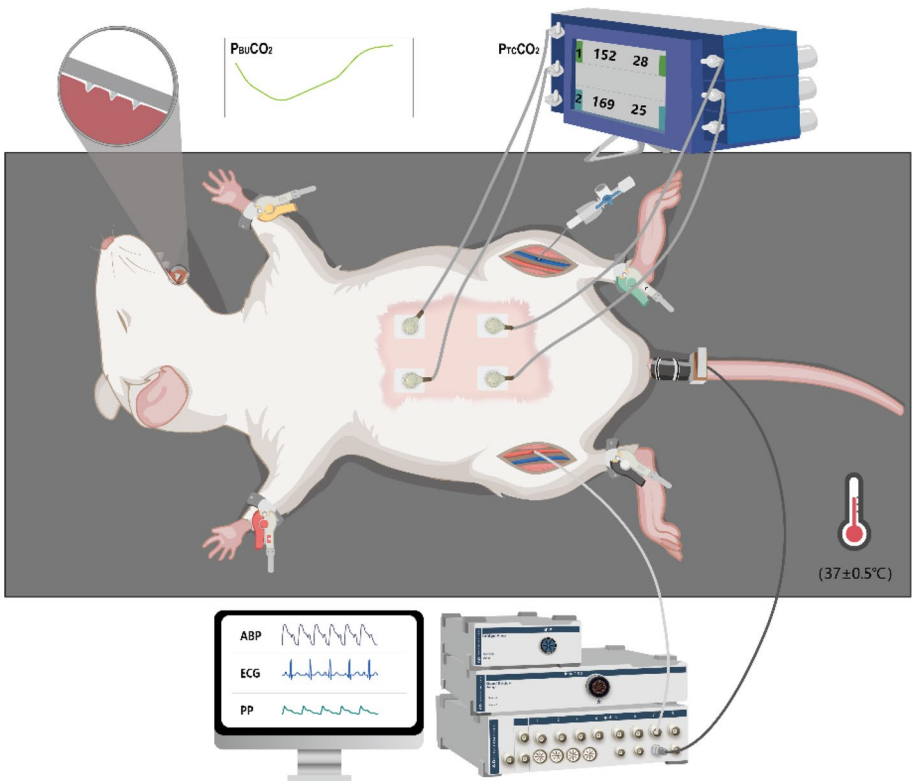

Fig. 6 Animal surgical scheme

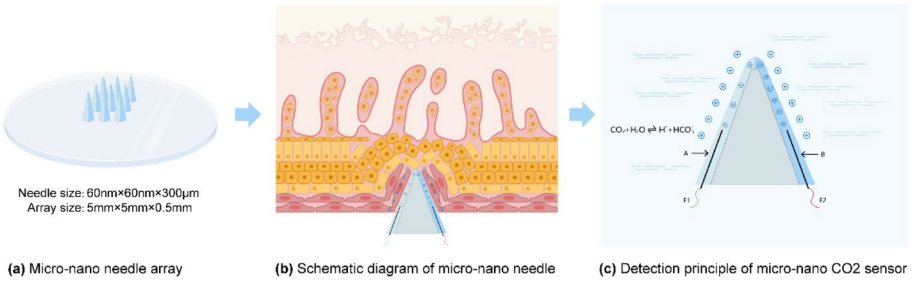

Fig. 7 Schematic diagram and detection mechanism of the micro-nano CO_2 sensor

bioelectrical amplification module, the pressure sensor was connected to the bridge amplification module, and the pulse sensor was connected to the main computer, in this order. The sensor was zeroed and calibrated by LabChart Pro8.0 software (AD Instruments, Bella Vista, Australia). The sampling frequency was selected as 1 kHz, the filtering frequency was 100 Hz, and the change in rat tail artery pulse pressure was taken as the measured value of PPV. The $P_{TC}O_2$ values from the four points in the abdomen of the rat were obtained in real time using a transcutaneous monitor (TCM400, Radiometer, Copenhagen, Denmark). The average of the four values was taken as the measured value of $P_{TC}O_2$.

Establishment of the multi-parameter prediction model based on the KNN and SVM algorithm

The KNN and SVM algorithms were implemented in Python 3.8.5 to establish a multi-parameter prediction model for the severity of hemorrhagic shock. The KNN algorithm, a nonparametric machine learning method with high classification accuracy [46], was employed to establish a multi-parameter hemorrhagic shock severity prediction model. Four physiological indices-MAP, $P_{BU}CO2$, $P_{TC}O_2$ and PPV-were defined as four-dimensional feature space inputs, with blood loss levels (25%, 30%, 35%, 40%) as classification labels. All experimental data was categorically labeled according to the amount of blood loss: data from groups with 0%, 25%, 30%, 35%, 40% are labeled with Categories 0–4, respectively. The generalized Euclidean distance function was used as the distance metric. To address sample size limitations, leave-one-out cross-validation was applied to optimize the hyperparameter K. For validation, a multi-parameter prediction model based on the SVM algorithm was developed. Similarly, all experimental data was categorically labeled according to the amount of blood loss: data from groups with 0%, 25%, 30%, 35%, 40% are labeled with Categories 0–4, respectively. A radial basis function was selected as the SVM kernel. Using the LibSVM toolbox [47], the training dataset was processed via the svmtrain function to establish the SVM-based multi-parameter prediction model. Both models were evaluated using confusion matrices to quantify classification performance (precision, recall, F1-score). For each model (KNN- or SVM- based), receiver operating characteristic (ROC) curves were generated for individual blood loss classes, with overall performance assessed via AUC value.

Statistical analysis

Data processing was performed using SPSS Statistics V25.0 software. Repeated measures ANOVA was performed, with repeated measurements at the different time points (15 min, 30 min, 45 min and 60 min after blood loss) as the dependent variable, and the groups (0%, 25%, 30%, 35%, and 40%) as the independent variable. Tukey's post hoc test was performed to test significant difference between different blood loss groups. The performance of the model was evaluated by using indicators such as accuracy, precision, recall, score, AUC, and ROC. Statistical results are expressed as mean ± SD, and $p \leq 0.05$ (bilateral) was considered statistically significant.

Abbreviations

HS	Hemorrhagic shock
HR	Heart rate
CO	Cardiac output
ABL	Arterial blood lactic acid
PPV	Pulse pressure difference
CRI	Compensated reserve index
$P_{BU}CO_2$	Buccal mucosal CO_2 partial pressure
LR	Logistic regression
NN	Neural networks
RF	Random forest
SVM	Support vector machine
LC	Blood lactate concentration
NI	New hemorrhage-induced severity index (NI = LC/PI)
PI	Perfusion index
DBP	Diastolic blood pressure
MAP	Mean arterial blood pressure
PPG	Photoplethysmography
$P_{TC}O_2$	Transcutaneous oxygen partial pressure
KNN	K-nearest neighbor algorithm
SPF	Specific pathogen-free
ECG	Electrocardiogram
MEMS	Micro-electromechanical systems
AUC	Area under ROC curve
HPV	Heart period variability
LBNP	Lower body negative pressure
RBF	Radial basis function
ROC	Receiver operating characteristic

Author contributions

Study conceptualization: Peng Zhao, Wencai Pan, Prediction Model Design and Implementation: Wencai Pan, Shihui Zhang, Animal Experiments: Jiaqing Yang, Yang Li, Project Supervision: Peng Zhao, Yufei Liu, Manuscript Drafting: Xin Zou, Manuscript Review and Editing: Peng Zhao.

Funding

This work was supported by the National Natural Science Foundation of China (81401487), the Chongqing Special Social Undertakings and People's Livelihood Security Science and Technology Innovation (cstc2016shmszx130082).

Availability of data and materials

No datasets were generated or analysed during the current study.

Declarations

Ethics approval and consent to participate

All animal-related procedures were conducted in strict compliance with the ethical standards approved by the Laboratory Animal Welfare and Ethical Committee of the Army Medical University.

Consent for publication

All the author consent for publication.

Competing interests

The authors declare no competing interests.

Received: 7 April 2025 Accepted: 6 May 2025
Published online: 20 May 2025

References

1. Yao Z, et al. Hemorrhagic shock assessed by tissue microcirculatory monitoring: a narrative revieW. Shock. 2024;61(4):509–19.
2. D'Orsi L, et al. A mathematical model of cardiovascular dynamics for the diagnosis and prognosis of hemorrhagic shock. Math Med Biol. 2021;38(4):417–41.
3. Curcio L, D'Orsi L, De Gaetano A. Seven Mathematical Models of Hemorrhagic Shock. Comput Math Methods Med. 2021;2021:6640638.
4. Latimer AJ, et al. The compensatory reserve index for predicting Hemorrhagic shock in prehospital trauma. Shock. 2023;60(4):496–502.
5. Feihl F, Waeber B, Liaudet L. The hemodynamics of septic shock: a historical perspective. Curr Vasc Pharmacol. 2013;11(2):133–8.
6. Coggins AR, et al. Utility of venous blood gases for the assessment of traumatic shock: a prospective observational study. Emerg Med J. 2021;38(9):711–7.
7. Norris PR, et al. Heart rate variability predicts trauma patient outcome as early as 12 h: implications for military and civilian triage. J Surg Res. 2005;129(1):122–8.
8. Cooke WH, et al. Autonomic compensation to simulated hemorrhage monitored with heart period variability. Crit Care Med. 2008;36(6):1892–9.
9. Jentzer JC, et al. Noninvasive hemodynamic characterization of shock and preshock using echocardiography in cardiac intensive care unit patients. J Am Heart Assoc. 2023;12(22): e031427.
10. Liaudet L, Waeber B, Feihl F. The hemodynamics of septic shock: a historical perspective. Curr Vasc Pharmacol. 2013. https://doi.org/10.2174/15701611380529017 3.
11. Convertino VA, et al. Compensatory reserve detects subclinical shock with more expeditious prediction for need of life-saving interventions compared to systolic blood pressure and blood lactate. Transfusion. 2021;61(1):S167-s173.
12. Di Carlo S, et al. Prehospital hemorrhage assessment criteria: a concise review. J Trauma Nurs. 2021;28(5):332–8.
13. Convertino VA, et al. Physiological comparison of hemorrhagic shock and V˙ O(2)max: A conceptual framework for defining the limitation of oxygen delivery. Exp Biol Med (Maywood). 2019;244(8):690–701.
14. Cammarata GA, et al. Buccal capnometry for quantitating the severity of hemorrhagic shock. Shock. 2009;31(2):207–11.
15. Lu H, et al. Buccal partial pressure of carbon dioxide outweighs traditional vital signs in predicting the severity of hemorrhagic shock in a rat model. J Surg Res. 2014;187(1):262–9.
16. Khajehpour H, Behzadnia MJ. The role of internal jugular vein Doppler ultrasonography in predicting hypovolemic shock in polytrauma patients. Ultrasonography. 2022;41(2):317–24.
17. Zhang G, et al. An interpretable deep learning algorithm for dynamic early warning of posttraumatic hemorrhagic shock based on noninvasive parameter. Biomed Signal Process Control. 2022;77: 103779.
18. Huang N, et al. Middle-level feature fusion for lightweight rgb-d salient object detection. IEEE Trans Image Process. 2022;31:6621–34.
19. Zhai S, et al. A "dual-key-and-lock" platform for distinguishing autophagy during neuroinflammation. Biosens Bioelectron. 2024;258: 116344.
20. Kim KA, et al. Mortality prediction of rats in acute hemorrhagic shock using machine learning techniques. Med Biol Eng Comput. 2013;51(9):1059–67.
21. Choi SB, et al. Prediction of ATLS hypovolemic shock class in rats using the perfusion index and lactate concentration. Shock. 2015;43(4):361–8.
22. Reljin N, et al. Using support vector machines on photoplethysmographic signals to discriminate between hypovolemia and euvolemia. PLoS ONE. 2018;13(3): e0195087.
23. Wong MKF, et al. Applied machine learning for blood pressure estimation using a small, real-world electrocardiogram and photoplethysmogram dataset. Math Biosci Eng. 2023;20(1):975–97.
24. Lou Z, et al. Near-infrared organic photodetectors toward skin-integrated photoplethysmography-electrocardiography multimodal sensing system. Adv Sci (Weinh). 2023;10(36): e2304174.
25. Pan WC, L.M., Zhao P, Song XY, Zhang X, Zhong YB, Lang L, Ma JS, Wang Q, Xu C, *The prediction of hemorrhagic shock severity based on multi-parameters with support vector machine.* In The 25th Annual Conference of China Medical Equipment Association. Guizhou, China, 2016.07: p. pp 1–5
26. Convertino VA, et al. Physiological and medical monitoring for en route care of combat casualties. J Trauma Injury, Infect Crit Care. 2008;64:S342–53.
27. Antonelli M, et al. Hemodynamic monitoring in shock and implications for management international consensus conference, Paris, France, 27–28 April 2006. Intensiv Care Med. 2007;33(4):575–90.
28. Stonko DP, et al. The underlying cardiovascular mechanisms of resuscitation and injury of REBOA and partial REBOA. Front Physiol. 2022;13: 871073.
29. Rickards CA, Tzeng YC. Arterial pressure and cerebral blood flow variability: friend or foe? A review Front Physiol. 2014;5:120.
30. Pestel GJ, et al. Assessing intravascular volume by difference in pulse pressure in pigs submitted to graded hemorrhage. Shock. 2006;26(4):391–5.
31. Butterfield ED, et al. Prehospital invasive arterial blood pressure monitoring in critically ill patients attended by a UK helicopter emergency medical service- a retrospective observational review of practice. Scand J Trauma Resusc Emerg Med. 2024;32(1):20.
32. Sharawy N, et al. Clinical relevance of early sublingual microcirculation monitoring in septic shock patients. Clin Hemorheol Microcirc. 2018;68(4):347–59.
33. Sircan-Kucuksayan A, et al. Investigating spectroscopic measurement of sublingual veins and tissue to estimate central venous oxygen saturation. Technol Health Care. 2022;30(3):541–9.
34. Soller BR, et al. Lightweight noninvasive trauma monitor for early indication of central hypovolemia and tissue acidosis: a review. J Trauma Acute Care Surg. 2012;73(1):S106–11.

35. Zhao P, Zheng JW, et al. Correlation between partial pressure of carbon dioxide in oral mucosa and degree of hemorrhagic shock in rats. Chin Sci Life Sci. 2011;10:230–7.
36. Alimjan, G., et al., A New Technique for Remote Sensing Image Classification Based on Combinatorial Algorithm of SVM and KNN. 2018. **32**(07): 1859012
37. Dou B, et al. Machine learning methods for small data challenges in molecular science. Chem Rev. 2023;123(13):8736–80.
38. Cannon JW. Hemorrhagic shock. N Engl J Med. 2018;378(4):370–9.
39. Liu J, et al. Automated analysis of vital signs to identify patients with substantial bleeding before hospital arrival: a feasibility study. Shock. 2015;43(5):429–36.
40. Angele MK, Schneider CP, Chaudry IH. Bench-to-bedside review: latest results in hemorrhagic shock. Crit Care. 2008;12(4):218.
41. Qasim Z. Resuscitative endovascular balloon occlusion of the Aorta: a practical review. Emerg Med Clin North Am. 2023;41(1):71–88.
42. Chiarelli AM, et al. Deep learning for hybrid EEG-fNIRS brain-computer interface: application to motor imagery classification. J Neural Eng. 2018;15(3): 036028.
43. Bermejo-Peláez D, et al. Classification of interstitial lung abnormality patterns with an ensemble of deep convolutional neural networks. Sci Rep. 2020;10(1):338.
44. Zhang Z, et al. Predictive analytics with ensemble modeling in laparoscopic surgery: a technical note. Laparosc Endosc Robot Surg. 2022;5(1):25–34.
45. Lee HB, Blaufox MD. Blood volume in the rat. J Nucl Med. 1985;26(1):72–6.
46. YB, S., Research on classification algorithm based on K nearest neighbors. 2009, Chongqing Univercity.
47. Chang CC, Lin CJ. LIBSVM: a library for support vector machines. Acm Trans Intell Syst Technol. 2011;2(3):27.

Publisher's Note